JOURNAL OF OPTOELECTRONICS AND ADVANCED MATERIALS Vol. 12, No. 4, April 2010, p. 895 - 899

Preparation and characterization of Mn-doped ZnO thin films

G. G. RUSU, P. GORLEY[a], C. BABAN, A. P. RAMBU, M. RUSU
Faculty of Physics „Al. I. Cuza" University, 11 Carol I Bldv, RO-700506, Iasi, Romania
[a]Yuri Fedkovych Chernivtsi National University, 2 Kotsyubynsky str., Chernivtsi, 58012, Ukraine

The Mn doped ZnO thin films (5.9 wt. %) (d = 140 – 300 nm) were prepared by thermal oxidation in ambient conditions, at 775 K, of the multilayered Zn/Mn thin stacks deposited in vacuum onto glass substrates by a modified version of two source evaporation technique. The XRD investigations revealed that the as doped ZnO films present a polycrystalline wurtzite structure with the predominant orientation of plane (002) parallel to the substrate surface. In respect of non-doped ZnO thin films, those Mn doped present a lower optical transmittance and an increase of the optical band gap. The temperature dependence of electrical conductivity (of about 1.6×10^{-6} $\Omega^{-1}.cm^{-1}$ at room temperature) of heat treated Mn doped ZnO films presents semiconducting characteristics.

(Received April 7, 2010; accepted April 26, 2010)

Keywords: Doped zinc Oxide, Thin films, X-ray diffraction, Optical properties, Electrical properties

1. Introduction

In the last decade, the interest for the behavior of the doped ZnO thin films has been considerable increased due to the multiple possibilities to influence their physical properties by nature and concentration of dopants. This interest is related to a great variety of the important applications of these films in optoelectronic devices, such as a conductive windows, gas sensors, optical wave guides, varistors, etc. [1]. In addition to these, the possibility to combine ferromagnetic and semiconducting properties of the transition-metal-doped ZnO thin films makes them very attractive for room temperature spintronic applications [2, 3]. Such as dilute magnetic semiconductor (DMS) materials have drawn considerable interest in the recent years. One of the most extensively studied DMS is Mn-doped ZnO.

A variety of preparation techniques have been reported to obtain pure and Mn doped ZnO thin films, such as pulsed laser deposition [4-8], r.f. magnetron sputtering [9, 10], atomic laser deposition [3], sol-gel [11-13], molecular beam epitaxy [14], etc. One of other technique by which can prepare ZnO thin films is the thermal oxidation of vacuum deposited metallic Zn films [15-17]. On the other hand, a deposition technique which can assure a uniform doping of a thin film is the multistacked layer method. We successfully used this method to prepare uniform Cu doped CdTe thin films by thermal activation of the interdifusion between adjacent layers of vacuum evaporated multilayered CdTe/Cu thin films [18]. In present paper, we investigate the possibility to combine these last two methods to obtain Mn-doped ZnO thin films by thermal oxidation in ambient conditions of vacuum evaporated multilayered Zn/Mn thin films. The structural, optical and electrical characteristics of as obtained doped ZnO thin films are studied.

2. Experimental

To obtain Mn-doped ZnO thin films, nanolayered Zn/Mn thin films were firstly deposited in vacuum onto cleaned glass substrates using multi-stacked layers method. The experimental procedure for growing Zn/Mn structures is the same as described previously [18-20]: metallic Zn and Mn powders were evaporated from independent separated sources maintained during film deposition at temperatures of 740 K and 1120 K respectively. During deposition, the glass substrates, fixed to a rotating disk, passed alternately over each evaporation source. The distance between sources and film substrates was about 6 cm. Using a special mask, both Zn and Mn reference samples were prepared simultaneously with Zn/Mn multilyered films. Other details of the experimental method and experimental setup are given in [20].

After deposition, using an automated Barnstead F21100 tube furnace, the as-grown Zn/Mn structures and reference samples were annealed in ambient condition by heating up to the temperature of 770 K with a constant rate of 8 K/min, maintained at this temperature for 20 min and subsequently cooling down to room temperature with the same rate.

The film thicknesses, d, ranging between 140 nm and 300 nm, were evaluated using the Fizeau's method for fringes of equal thicknesses using an interferential microscope. By taking into account the thicknesses of both Zn and Mn reference samples, the weigh ratio Mn:Zn in the as deposited Zn/Mn thin films was estimated as 5.9 wt.%.

The structural characteristics of as deposited and thermal oxidized samples were investigated using XRD measurements with CuK_α radiation (λ = 1.5418 Å).

For the optical studies, normal reflectance, *R*, and transmittance, *T*, corrected for the effect of the glass substrates were recorded in the 200 nm and 1700 nm wavelength range using a Tec5 computer controlled spectrometer.

The behavior of the electrical conductivity of the studied samples was investigated by measuring their electrical resistance in the temperature range 300 K – 600 K, using surface type cell. For electrical contacts, silver vacuum evaporated electrodes, separated by a gap of 3 mm, were used.

3. Results and discussion

3.1. Structural characterization

The XRD patterns, both for as-deposited samples and heat-treated Mn doped ZnO thin films are shown in Fig.1. From Fig. 1a, b one can observe that both as-deposited and heat-treated doped samples are polycrystalline. The XRD pattern of the as-deposited sample (Fig. 1a) exhibits the diffraction peaks characteristic both for Zn and Mn crystalline bulks. The peaks from 2θ of 36.8º, 43.3º and 54.5º correspond to (002), (101) and (102) planes, respectively, of hexagonal wurtzite crystalline structure of Zn bulk [21] whereas, the peaks from 2θ of 40.5º, 43.0º and 56.6º are characteristic for cubic Mn structure [22]. The annealing of as-deposited Zn/Mn samples up to temperature of about 770 K determines the oxidation of respective films with formation of ZnO compound having the hexagonal wurtzite crystalline structure [23]. The weak peaks at 2θ of 43.3º and 54.5º respectively, from Fig. 1b suggest that in the respective sample, a small Zn amount remained non-oxidized. No additional diffraction peaks which would correspond to other Mn related phases as results of the annealing process, detectable by XRD measurements, was observed, suggesting that Mn was incorporated in the ZnO lattice. The absence of the oxide phases of Mn in $Zn_{1-x}Mn_xO$ films prepared by pulsed laser deposition has been also reported [24, 25].

Comparing the peak intensities from Fig. 1b with the standard one [23], the prevalence of the (002) texture was revealed. The preferred crystallite orientation in the studied Mn doped ZnO thin films was evaluated using the texture coefficient $TC_{(hkl)}$ defined as [26, 27]:

$$TC_{(hkl)} = \frac{I_{hkl}/I_{0hkl}}{(1/n)\sum_n I_{hkl}/I_{0hkl}} \quad , \qquad (1)$$

where I_{hkl} and I_{0hkl} denote the relative measured and ASTM standard XRD intensities of (hkl) peaks, respectively, and *n* is the number of the considered diffraction peaks. In Table 1, the values of texture coefficient calculated for the main diffraction peaks from Fig. 1b are summarized. One can be seen that respective $TC_{(hkl)}$ values are deviated from unity value (corresponding to non-textured sample) especially that for (002) peak. This fact confirms the preferred c-axis orientation of crystallites in respective films. Similar (002) texture was reported for other Mn doped ZnO thin films [9].

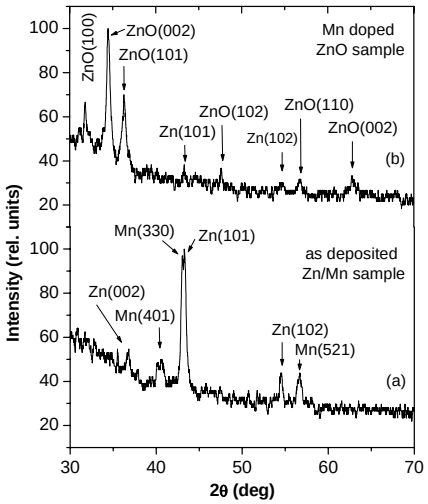

Fig. 1. Typical XRD patterns for studied samples: (a) –as deposited Zn/Mn sample, (b) – Mn-doped ZnO sample.

Table 1. Some structural characteristics for Mn doped ZnO thin films: $TC_{(hkl)}$ - texture coefficient; D - crystallite size; a_0, c_0 - standard cell parameters; a, c- experimental cell parameters.

(hkl) plane	$TC_{(hkl)}$	*D* (nm)	a_0 (Å)	*a* (Å)	c_0 (Å)	*c* (Å)
(100)	0.50	36.1	3.249	3.259	5.206	5.208
(002)	1.99	20.8				
(101)	0.50	20.0				

Using the X-ray diffraction data, the interplanar distances and the lattice parameters *a* and *c* were calculated for thermal oxidized samples. As can observe from Table 1, the obtained values for cell parameters are slightly grater than standard ones. This indicates that Mn doping can determine some lattice disturbance in ZnO samples. Such increased lattice parameters of Mn-doped ZnO thin films was also reported in literature and was connected with ionic radii difference between zinc and manganese ions [5, 14, 28-30].

Using the Scherrer's formula [31]:

$$D = \frac{0.9 \cdot \lambda}{\beta \cdot \cos\theta} \quad , \qquad (2)$$

where λ, θ and β are the X-ray wavelength (1.5418 Å), Bragg diffraction angle and full-width at half maximum (FWHM) of diffraction peak, respectively, the crystallite size of oxidized Mn doped ZnO thin films were evaluated. The obtained values of crystallite size along the main

diffraction planes are listed in Table 1. The average crystallite size of about 25 nm indicates the nanocrystalline structure of respective films.

3.2. Optical characteristics

The study of the optical properties of Mn-doped semiconducting oxides are important in the magneto-optic applications of respective films. In this paper, the transmission and absorption spectra of non-doped and Mn-doped ZnO films were investigated. The typical transmission spectra of the studied films are shown in Fig. 2.

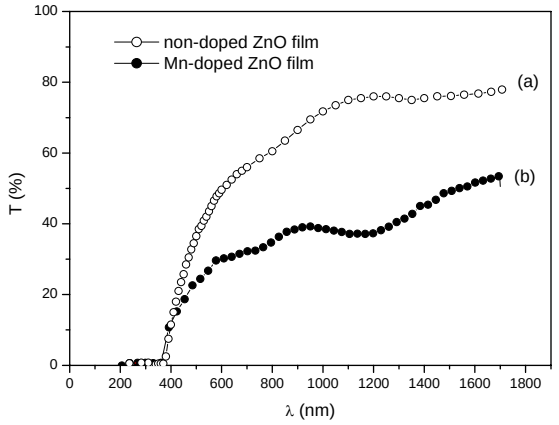

Fig. 2. Typical transmission spectra for studied films.

As it results from the respective figure, the presence of Mn ions in ZnO samples determines a decrease of film transmittance with respect to those of non-doped ZnO films. For a better comparison, the values of absorption coefficient, α, near the fundamental absorption edge, for the respective samples were calculated, using the relation [32]:

$$\alpha = \left(\frac{1}{d}\right)\ln\left[\frac{(1-R)^2}{T}\right] \quad , \tag{3}$$

where d is the film thickness and R and T are the film reflectance and transmittance, respectively. In Fig. 3(inset), the respective absorption spectra are plotted. The greater absorbance of Mn doped sample can be associate both with the loss of light by scattering at grain boundaries and weaker crystallinity of the doped sample.

The ZnO crystals are characterized by direct allowed transitions [33, 34]. In this case, the relation between α and optical band gap, E_g, is given by the relation [32, 35]:

$$\alpha h\nu = A\left(h\nu - E_g\right)^{1/2} \quad , \tag{4}$$

where A is a parameter independent on the photon energy, hν. By extrapolating the linear portion of the $(\alpha h\nu)^2 = f(h\nu)$ dependence to $(\alpha h\nu)^2 \to 0$, the values of optical band gap were determined for the investigated samples. As it results from Fig. 3, the absorption band edge for Mn-doped sample is shift toward higher photon energy compared with non-doped ones, indicating an increase of the optical band gap of respective film.

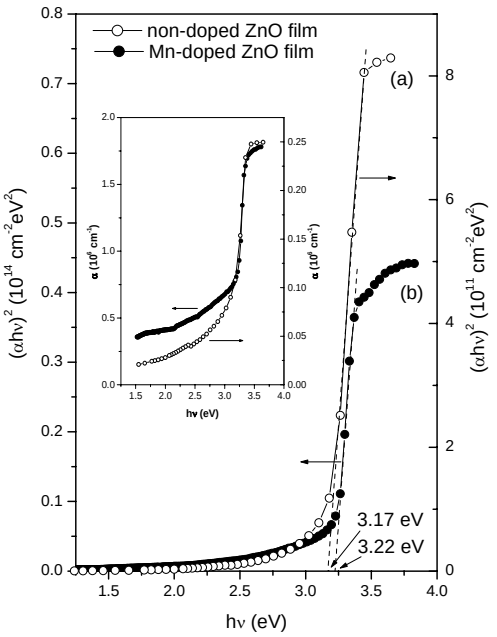

Fig. 3. Plot of $(\alpha h\nu)^2$ vs. hν and α vs. hν (inset) for typical studied samples: (a) – non-noped ZnO sample, (b) – Mn-doped ZnO sample.

The increase of the optical band gap with from 3.27 eV to 3.52 eV with increase of Mn content from $x = 0$ to $x = 0.25$ in $Zn_{1-x}Mn_xO$ thin films has been also observed by Mandel and Nath for Mn doped ZnO epitaxial films growen by pulsed laser deposition techniques onto (0001) sapphire substrates [36]. Many other researchers [3, 5, 7, 12-14, 24, 28, 37] reported the blue shift of the fundamental absorption edge with increase of Mn content in doped ZnO films and the presence of an additional absorption band in front of absorption edge. These optical behaviors were attributed mainly to the sp-d spin exchange interaction between the band electrons and localized d electrons of Mn^{+2} ions. In the case of our studied samples, the observed absorption edge blue shift of doped sample is relative lower. In addition, the calculated value of E_g for non-doped film is lower than 3.28 eV – 3.30 eV indicated in the literature data. This relative lower value (of about 3.17 eV) obtained for our non-doped ZnO thin films can be due to the greater density of donor states near the conduction band determined mainly by the oxygen deficiency and structural defects produced by Mn incorporation during thermal oxidation process. These acts as n-type donor impurities [38, 39] and consequently, a density of state tail extended into forbidden band can

appear [32], determining a reduction of the effective band gap. This fact can also mask the blue shift of absorption edge for our samples, if this there is for respective films.

3.3. Electronic transport properties

The literature data regarding the electrical properties of Mn doped ZnO thin films show that the electrical resistivity of these films varied in a large limits from about 10^{-2} Ω.cm up to approximately 10^{6} Ω.cm [7, 9, 14, 28]. This fact indicates that the electrical properties of Mn doped ZnO films are strongly dependent on the structural characteristics of respective films, which, in turn, depend on the preparation conditions.

In Fig. 4, the typical temperature dependence of electrical conductivity for studied Mn doped ZnO films are plotted. Before electrical measurements, the respective samples were subjected to a heat treatment consisting of several successive heating/cooling cycles, in the temperature range 300 K – 600 K in order to stabilize their structures. The removal of some adsorbed and absorbed gases and the reduction of the structural defects and impurity concentration may occur during such heat treatment. As it results from Fig. 4, the respective samples have a semiconducting behavior of electrical conductivity versus reciprocal temperature in concordance with the relation [40]:

$$\sigma = \sigma_0 \exp\left(-\Delta E / 2kT\right) \quad , \qquad (5)$$

where ΔE denotes the thermal activation energy of electrical conduction, σ_0 is a parameter depending on the compound nature and k is Boltzmann constant. From the slope of the curve plotted in Fig. 4 for higher temperature domain, where, usually, the intrinsic conduction prevail, the value of ΔE of 1.10 eV for Mn doped ZnO films was calculated.

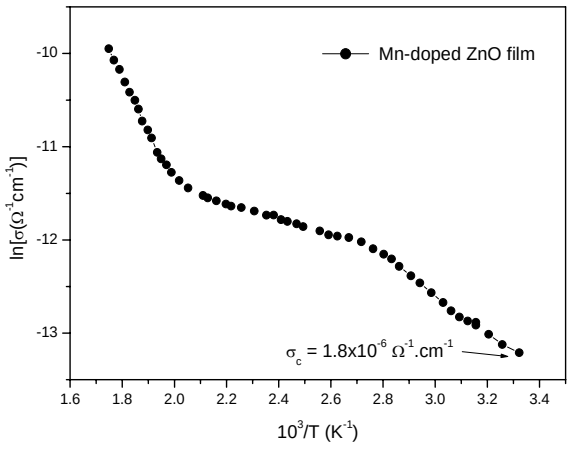

Fig. 4. Typical temperature dependence of electrical conductivity for Mn-doped ZnO thin films (σ_c – electrical conductivity at room temperature).

The lower value of electrical conductivity can be correlated with the nanogranular structure of the film. The grain size, their shape and the potential barriers at their interface strongly influence the charge carrier transport, especially their mobility [41]. The decrease of carrier mobility in the doped ZnO films was also reported by other researchers [7, 28]. The decrease of carrier concentration as consequence of the electrical compensation in the material and the carrier localization may also determine the increase of electrical resistivity of the films [14].

Regarding the magnetic properties of the studied films, the preliminary investigations indicate that, at room temperature, these samples are non magnetic.

4. Conclusions

In the present paper, the possibility to obtain uniform Mn-doped ZnO thin films by thermal oxidation of evaporated multilayered Zn/Mn thin films was demonstrated. The XRD analysis revealed that as prepared Mn-doped ZnO thin films have a polycrystalline wurtzite structure with (002) plane of crystallites parallel to the substrate surface. The optical band gap evaluated from $\left(\alpha h\nu\right)^2 = f\left(h\nu\right)$ dependences was found to be of 3.17 eV and 3.22 eV for non-doped and doped samples, respectively.

The temperature dependence of electrical conductivity of heat treated Mn doped samples present a semiconducting characteristics, with activation energy of electrical conduction, in the higher temperature range of about 1.10 eV.

At room temperature, the studied samples have no magnetic properties.

Acknowledgements

Part of this work was done under financial support of the grant CNCSIS 76CB/30.07.2008.

References

[1] H. L. Hartnagel, A. L. Dawar, A. K. Yain, C. Jajadish, Semiconducting Transparent Thin Films, Inst. of Publishing, Bristol, 1995.
[2] T. Diethl, O. Ohno, F. Matsukura, J. Cibert, D. Ferrand, Science, **287**, 1019 (2000).
[3] M. Godlewski, A. W-Glodowska, E. Guziewicz, S. Yatsunenko, A. Zakrzewski, Y. Dumont, E. Chikoidze, M. R. Phillips, Opt. Mater.doi 10.1016/j.optmat.2008.12. 031.
[4] G. Brauer, W. Anwand, W. Skorupa, H. Schmidt, M. Diaconu, M. Lorenz, M. Grundmann, Superlatt. Microstruct. **39**, 41 (2006).
[5] S. Karamat, S. Mahmood, J. J. Lin, Z. Y. Pan, P. Lee, T. L. Tan, S. V. Springham, R. V. Ramanujan, R.S. Rawat, Appl. Surf. Sci., **254,** 7285 (2008).

[6] A. K. Pradhan, D. Hunter, K. Zhang, J. B. Dadson, S. Mohanty, T. M. Williams, K. Lord, R. R. Rakhimov, U. N. Roy, Y. Cui, A. Burger, J. Zhang, D.J.Sellmyer, Appl. Surf. Sci., **252,** 1628 (2005).
[7] P. Bhattacharya, R. Das, J. Nieves, Yu. I. Yuzyuk, R. S. Katiyar, Mat. Res. Symp. Proc. **764,** C3.20.1 (2003),
[8] M. Diaconu, H. Schmidt, H. Hochmuth, M. Lorenz, G. Benndorf, J. Lenzner, D. Spemann, A. Setzer, K-W. Nielsen, P. Esquinazi, M. Grundman, Thin Solid Films, **486**, 117 (2005).
[9] C. Liu, F. Yun, B. Xiao, S-J. Cho, Y. T. Moon, H. Morkoc, M. Abouzaid, R. Ruterana, K. M. Yu, W. Walukiewicz, J. Appl. Phys., **97**, 126107 (2005).
[10] C. Liu, B. Xiao, F. Yun, H. Lee, U. Ozgur, Y. T. Moon, H. Morkoc, M. Abouzaid, P. Ruterana, Superlatt. Microstruct. **39**, 124 (2006).
[11] Y. M. Kim, M. Yoon, I. W. Park, J. H. Lyou, Solid State Commun., **129**, 175 (2004).
[12] M. Yuonesi, M. E. Ghazi, M. Izadifard, M. Yaghobi, J. Opoelectron. Adv. Mater., **10**(10), 2603 (2008).
[13] G. Srinivasan, J. Kumar, J. Crys. Growth, 310, 1841 (2008).
[14] V. Avrutin, N. Izyumskaya, U. Ozgur, A. El-Shaer, H. Lee, W. Schoch, F. Reuss, V. G. Beshenkov, A. N. Pustovit, A. Che Mofor, A. Bakin, H. Morkoc, A. Waag, Superlatt. Microstruct., **39**, 291 (2006).
[15] J. Zhao, L.Hu, Z. Wang, Y. Zhao, X. Liang, M. Wang, Appl. Surf. Sci., **229**(1- 4), 311 (2004).
[16] R. K. Gupta, N. Shridhar, M. Katiyar, Materials Science in Semicond. Processing, **5**(1), 11 (2002).
[17] G. G. Rusu, M. Rusu, N. Apetroaei, Thin Solid Films, **515**, 8699 (2007).
[18] G. G. Rusu, M. Rusu, J. Optoelectron. Adv. Mater., **7**(2), 885 (2005).
[19] G. G. Rusu, M. Rusu, M. Gîrtan, Vacuum **81,** 1476 (2007).
[20] G. G. Rusu, A. P. Râmbu, M. Rusu, J. Optoelectron. Adv. Mater., **10**(2), 339 (2008).
[21] Joint Committee on Powder Diffraction Standards, Powder Diffraction File, card no. 04-0831.
[22] Joint Committee on Powder Diffraction Standards, Powder Diffraction File, card no. 32-0637.
[23] Joint Committee on Powder Diffraction Standards, Powder Diffraction File, card no. 36-1451.
[24] T. Fukumura, Z. Jin, A. Ohtomo, H. Koinuma, M. Kawasaki, Appl. Phys.Lett. **75,** 3366 (1999).
[25] H. K. Yadav, K. Sreenivas, V. Gupta, J. Appl. Phys., **99,** 083507 (2006).
[26] C. S. Barret, T. B. Massalski, Structure of Metals, Pergamon Press, Oxford, 1980, p. 204.
[27] A. A. Ramadan, A. A. Abd El-Mongy, A. M. El-Shabiny, A. T. Mater, S. H. Mostafa, E. A. El-Sheheedy, H. M. Hashem, Cryst. Res. Technol., **44**(1), 111 (2009).
[28] E. Chikoidze, Y. Dumont, F. Jomard, O. Gorochov, Thin Solis Films, **515,** 8519 (2007).
[29] Y. Xia, F.Huang, W. Wang, Y. Wang, K. Yuan, M. Liu, J. Shi, Opt. Mater., **31,** 311 (2008).
[30] D. S. Reddy, S. K. Sharma, Y. D. Reddy, B. S. Reddy, K. R. Gunasekhar, P. S. Reddy, J. Opoelectron. Adv. Mater., **10**(10), 2607 (2008).
[31] B. D. Cullity, R. S. Stock, Elements of X-Ray Diffraction, Prentice Hall, 3rd ed, New Jersey, 2001.
[32] J. I. Pankove, Optical Processes in Semiconductors, Dover, New York, 1971.
[33] R. Bangava (Ed), Properties of wide bandgap II-VI semiconductors, EMIS Inspect London, 1997.
[34] C. Jagadish, S. J. Pearson (Eds), Zinc Oxide Bulk, Thin Films and Nanostructures; Processing, Properties and Applications, Elsevier, Amsterdam, 2006.
[35] N. F. Mott, E. A. Davis, Electronic Processes in Non-Crystalline Materials, Clarendon Press, Oxford, 1979.
[36] S. K.Mandal, T. K.Nath, Thin Solid Films **515,** 2535 (2006).
[37] Y. S. Wang, P. J. Thomas, P. O'Brien, J. Phys. Chem. B, **110** (43), 21412 (2006).
[38] G. Harbeke (Ed.), Polycrystalline Semiconductors. Physical Properties and Applications, Spring-Verlag, Berlin, 1985.
[39] Z. L. Wang, J. Phys. Condens. Matter **16**, R829 (2004).
[40] K. Seeger, Semiconductor Physics, Springer, Berlin, 1999.
[41] L. L. Kazmersky, Polycrystalline and Amorphous Thin Films and Devices, Academic Press, London, 1980.

*Corresponding author: rusugxg@uaic.ro